



# Caveolin-1-ACE2 axis modulates xenobiotic metabolism-linked chemoresistance in ovarian clear cell carcinoma

Arulkumar Nagappan · Ki-Hyung Kim ·  
Yuseok Moon

Received: 5 January 2022 / Accepted: 17 May 2022 / Published online: 27 May 2022  
© The Author(s), under exclusive licence to Springer Nature B.V. 2022

**Abstract** Among epithelial ovarian cancers, ovarian clear cell carcinoma (OCCC) remains markedly resistant to platinum-based chemotherapy, leading to poor clinical outcomes. In response to xenobiotic insults, caveolar platforms play crucial roles in modulating stress signaling responses in cancer cells. It has been hypothesized that caveolin-1 (Cav-1), a main component of the lipid raft, may regulate the response to platinum-based treatment in OCCC. The clinical transcriptomic evaluation

demonstrated that high Cav-1 expression was positively associated with a favorable prognosis in patients with ovarian cancer. Cav-1 overexpression enhanced sensitivity to cisplatin (CDDP) treatment, whereas Cav-1 deficiency promoted chemoresistance in OCCC cells. Mechanistically, although Cav-1 counteracted angiotensin-converting enzyme 2 (ACE2) expression, ACE2 positively facilitated resistance to CDDP in OCCC cells. Furthermore, ACE2 restricted aryl hydrocarbon receptor expression and subsequent transcription of drug-metabolizing enzymes. Of note, ACE2 positively regulated the expression of the platinum-clearing enzyme CYP3A4. These findings suggest that the Cav-1-ACE2 axis modulates xenobiotic metabolism-linked chemoresistance in OCCC, predicting potential roles for the stress sentinel networks in oncogenic processes.

Arulkumar Nagappan and Ki-Hyung Kim contributed equally to this paper.

## Graphical highlights

- Cav-1 is inversely associated with chemoresistance in OCCC cells.
- Cav-1-counteracted ACE2 is involved in OCCC resistance to cisplatin.
- ACE2 facilitates expression of CYP3A4, a key enzyme for platinum-based drug clearance.

**Supplementary Information** The online version contains supplementary material available at <https://doi.org/10.1007/s10565-022-09733-1>.

A. Nagappan · K.-H. Kim · Y. Moon (✉)  
Laboratory of Mucosal Exposome and Biomodulation,  
Department of Integrative Biomedical Sciences, Pusan  
National University, Yangsan 50612, Korea  
e-mail: moon@pnu.edu

K.-H. Kim  
Department of Obstetrics and Gynecology, College  
of Medicine, Pusan National University, Busan, Korea

**Keywords** Ovarian clear cell carcinoma ·  
Caveolin-1 · Chemotherapy · Angiotensin-converting  
enzyme 2 · Aryl hydrocarbon receptor · Xenobiotic  
metabolism

K.-H. Kim · Y. Moon  
Biomedical Research Institute, Pusan National University  
Hospital, Busan, Korea

Y. Moon  
Graduate Program of Genomic Data Sciences, Pusan  
National University, Yangsan 50612, Korea

## Introduction

Epithelial ovarian cancer (EOC) is the most common cause of gynecological cancer-related deaths among women (Kim et al., 2016). Ovarian clear cell carcinoma (OCCC) is a distinct subtype of EOC, both biologically and clinically, accounting for 3.7–12.1% of all histological subtypes (Orezzoli et al., 2008). Among histological subtypes, patients with OCCC display poor sensitivity to first-line chemotherapy as well as poor clinical outcomes in advanced stages after recurrence (Ho et al., 2004). In particular, advanced-stage OCCC has a low response rate of only 11% to platinum-based chemotherapy, whereas serous adenocarcinoma affords a response rate of 72% (Sugiyama et al., 2000). As each EOC subtype exhibits unique features and discrete drug responses, specific interventions against potential targets of progression need to be developed to improve the prognosis of patients with OCCC.

Caveolin-1 (Cav-1) is an integral transmembrane protein that resides in major structural and functional components of specialized lipid raft microdomains, particularly plasma membrane invaginations called caveolae in various mammalian cell types (Fujimoto et al., 2000; Rothberg et al., 1992). Cav-1 interacts with diverse signaling molecules, which are associated with signal transduction, lipid transport, membrane trafficking, gene regulation, and tumor metastasis (Tirado et al., 2010a). The role of Cav-1 in cancer remains controversial owing to its dual functions as a tumor suppressor and promoter (Gupta et al., 2014). Cav-1 mediates the progression and metastasis of various cancer types (Chen et al., 2011; Wang et al., 2014; Xu et al., 2014). Furthermore, Cav-1 overexpression has been associated with chemoresistance in lung and breast cancers (Cai and Chen, 2004; Ho et al., 2008). In contrast, Cav-1 has been identified as a tumor suppressor in human ovarian carcinoma (Kai et al., 2001), although the role of Cav-1 in the progression, development, and chemoresistance of OCCC has not been established. Additionally, Cav-1 tyrosine phosphorylation augments the drug sensitivity of breast cancer cells (Shajahan et al., 2007). Cav-1 can interact with several signaling platforms of receptors, such as epidermal growth factor receptor (EGFR) and platelet-derived growth factor receptors (Vihanto et al., 2006). EGFR is considered a potential prognostic biomarker and therapeutic target for

ovarian cancer, as it is expressed in 30–98% of EOC (Gui and Shen, 2012). EGFR is an important signaling scaffold that critically regulates cell proliferation, migration, adhesion, and tumor angiogenesis (Gui and Shen, 2012). The interaction between Cav-1 and EGFR can suppress tyrosine phosphorylation and kinase activity and inhibit tumor cell proliferation and metastasis (Couet et al., 1997; Williams et al., 2004).

Lipid raft microdomains, including caveolae, are crucial platforms for viral entry and numerous physiological signaling pathways. Virus internalization into host cells is mediated via endocytic pathways such as clathrin- or caveolae-dependent endocytosis (Pelkmans, Helenius, 2003). Virus internalization is initiated by external ligand binding to receptors, including the angiotensin-converting enzyme 2 (ACE2) receptor (Hennighausen, Lee, 2020). The causative agent of coronavirus disease (COVID-19), severe acute respiratory syndrome coronavirus 2 (SARS-CoV-2), has been found to bind to the ACE2 receptor as a component of the renin-angiotensin system, which is a crucial physiological regulator of circulating angiotensin II (Ang II) (Khanna et al., 2021). Moreover, ACE2, as a pathophysiological sensor, plays a critical role in cancer angiogenesis (Zhang et al., 2019), chemoresistance in renal cell carcinoma (RCC) (Khanna et al., 2021), and cancer cell growth (Krishnan et al., 2013); however, the precise molecular mechanism through which ACE2 plays a role in chemoresponses remains poorly understood.

As another sentinel to external insults, the aryl hydrocarbon receptor (AhR) regulates biological and toxicological responses to environmental stress that modulate the expression of genes involved in xenobiotic metabolisms, such as cytochrome P450 (CYP) pathways (Stejskalova et al., 2011). Particularly, CYP3A4, the most abundant CYP in the human liver, is responsible for metabolizing more than 50% of clinical therapeutics including anticancer agents (Scripture et al., 2005). Mostly, CYP3A4 facilitates the systemic clearance of chemotherapeutic agents (Goldstein et al., 2013). Several epidemiological studies have suggested that AhR-CYP pathways are strongly associated with cancer initiation and progression (Deuster et al., 2019; Safe et al., 2013). Cancer cells can respond to environmental stressors, such as infectious agents and xenobiotic insults, by regulating the sentinel receptors. On an assumption that Cav-1 is a potent platform of stress-responsive receptors,

we assessed whether the receptor-linked network is involved in the regulation of chemoresponses. In particular, the sentinel signaling receptors including ACE2 and AhR were evaluated in terms of clinical response to chemoresistant ovarian cancers.

## Materials and methods

### Cell culture and chemical reagents

Human OCCC cell lines, including RMG-1, KOC7C, OVTOKO, TOV21G, and ES2 and A2780 type II human EOC cells, were kindly provided by Dr. Fumitaka Kikkawa (Department of Obstetrics and Gynecology, Nagoya University Graduate School of Medicine, Nagoya, Japan). ES2 cells were maintained in McCoy's 5A medium; all other cell lines were maintained in RPMI 1640 medium, supplemented with 20% (v/v) heat-inactivated fetal bovine serum (FBS), 50 U/mL penicillin, and 50 mg/mL streptomycin (all from Welgene, Daegu, Korea) in a 5% CO<sub>2</sub> humidified incubator at 37 °C. The trypan blue (Sigma-Aldrich, St. Louis, MO, USA) dye exclusion assay was performed to count the cell numbers using a hemocytometer. Cisplatin (CDDP) was obtained from Sigma-Aldrich. 3-(4,5-dimethylthiazol-2-yl)-2,5-diphenyltetrazolium bromide (MTT) powder was obtained from Duchefa Biochemie (BH Haarlem, Netherlands). Crystal violet was purchased from Biosesang Inc. (Seongnam, Korea). Primary antibodies against  $\beta$ -actin, Cav-1, EGFR, PAPR-1, p53, caspase-3, and AhR were purchased from Santa Cruz Biotechnology (Santa Cruz, CA, USA). Rabbit anti-ACE2 antibody was obtained from Abclonal, Inc. (Woburn, MA, USA).

### Analysis of survival and transcriptomic datasets

Datasets of ovarian cancers, GSE29450 ( $n=20$ ), GSE14407 ( $n=24$ ), GSE50831 ( $n=189$ ), GSE26193 ( $n=107$ ), and GSE63885 ( $n=101$ ), were retrieved from the public repository GEO database (<https://www.ncbi.nlm.nih.gov/geo/>), and mRNA profiles of targeted genes were analyzed. We used the cBioPortal online platform (<http://www.cbioportal.org/>) to analyze co-expressed genes predicted from mRNA data of ovarian serous cystadenocarcinoma (TCGA, Nature 2011, 489 patients). Kaplan–Meier

survival analysis was performed based on specific gene expression levels in patients with low-grade serous ovarian carcinoma (GSE27651,  $n=49$ ), high-grade human ovarian adenocarcinomas (OVA; GSE26193,  $n=107$ ), and ovarian cancer (GSE63885,  $n=101$ ) from the Kaplan–Meier plotter (for ovarian cancer) database (<https://kmplot.com/analysis/>).

### Cytotoxicity and clonogenic survival assays

OCCC cell lines were seeded onto 96-well plates at a density of 5000 cells/well and were cultured for 24 h. The medium was removed, and fresh medium or CDDP was added to attain a final volume of 200  $\mu$ L/well. After incubation for 24 h, the culture medium was removed, and 50  $\mu$ L of phosphate-buffered saline (PBS) containing 1 mg/mL MTT was added to each well and incubated for 4 h. Next, the PBS-containing MTT solution was carefully removed, and 100  $\mu$ L of dimethyl sulfoxide (DMSO) was added to each well and incubated for 15 min at 25 °C. Absorbance was measured at 540 nm using a microplate reader (Molecular Devices, Sunnyvale, CA, USA). The 50% inhibitory concentration (IC<sub>50</sub>) value of the cell viability was evaluated using CompuSyn 1.0 software (ComboSyn Inc., Paramus, NJ, USA).

For the clonogenic survival assay, cells were seeded onto 6-well plates at a density of 300–500 cells/well. Twenty-four hours after seeding, cells were treated with CDDP for 24 h. Cells were replaced with fresh medium every 2 days and were allowed to grow for 8–12 days. The cells were then fixed with 4% formaldehyde and were followed by staining with 0.5% crystal violet in a 25% methanol solution. Plates containing colonies were scanned using an Epson Perfection 3490 Photo Scanner (Epson America, Inc., Los Alamitos, CA, USA).

### Plasmid construction

Human cytomegalovirus (CMV) promoter-driven short hairpin RNA (shRNA) was generated by inserting shRNA templates into a pSilencer 4.1-CMVneo vector (Ambion, Austin, TX, USA). Inserts of CAV-1 and ACE2 shRNA targeted 5'-GCC CAA CAA CAA GGC CAT G-3' and 5'-AAC CAC GAA GCC GAA GAC CTG-3', respectively. The Flag-tagged Cav-1 construct was amplified using the following primers: 5'-CAC CAT GGA CTA CAA GGA CGA CGA TGA CAA GAT GGC AGA

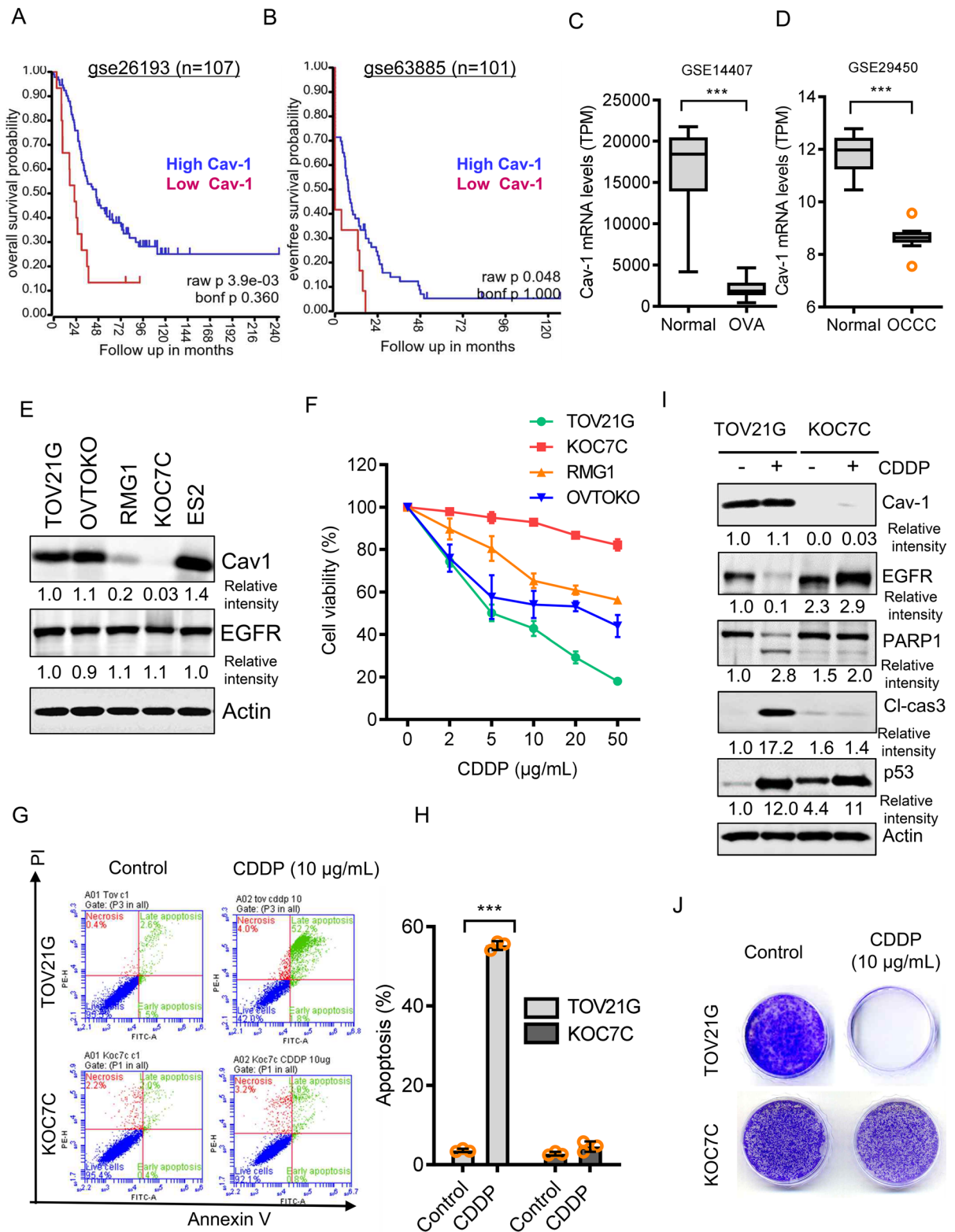


**Fig. 1** Cav-1 expression is inversely associated with sensitivity to cisplatin. **A, B** Kaplan–Meier plot of overall survival (OS) analysis for patients with high and low expression of Cav-1 from the GSE26193 (**A**,  $n=107$ ) and GSE63885 datasets (**B**,  $n=101$ ). **C** *CAV-1* mRNA expression profiles of ovarian adenocarcinoma (OVA) and normal ovarian tissue were obtained from the GSE14407 dataset (normal,  $n=12$ ; OVA,  $n=2$ ). **D** *CAV-1* mRNA expression profiles of OCCC and normal ovarian tissue were obtained from the GSE29450 dataset (normal,  $n=10$ ; OCCC,  $n=10$ ). Asterisks (\*) indicate significant differences ( $***p<0.001$ ) compared with the normal group. **E** Basal protein expression of Cav-1 and EGFR in OCCC cell lines was determined by immunoblotting analysis. **F** The sensitivity of OCCC cell lines to cisplatin was measured using the 3-(4, 5-dimethylthiazol-2-yl)-2, 5-diphenyltetrazolium bromide (MTT) assay. OCCC cells were treated with the indicated concentrations of cisplatin for 24 h, and a cell viability assay was performed. **G, H** TOV21G and KOC7C cells were treated with vehicle or 10  $\mu\text{g}/\text{mL}$  cisplatin for 24 h and were stained with annexin V–fluorescein isothiocyanate (FITC) and propidium iodide (PI). The proportion of apoptotic cells was measured by using BD Accuri™ C6 Plus flow cytometer, and data are shown as the mean  $\pm$  standard deviation (SD) of three independent experiments ( $***p<0.001$  vs. vehicle group). **I** TOV21G and KOC7C cells were treated with vehicle or 10  $\mu\text{g}/\text{mL}$  cisplatin for 24 h, and total cell lysates were subjected to immunoblotting analysis. Representative images are shown. **J** Clonogenic cell survival assay of TOV21G and KOC7C cells. The cells were treated with vehicle or 10  $\mu\text{g}/\text{mL}$  cisplatin for 24 h, cultured in fresh medium for 8 to 12 days, and then stained with crystal violet. Representative images are shown. Cav-1, caveolin 1; Cl-cas3, Cleaved Caspase-3; EGFR, epidermal growth factor receptor; OCCC, ovarian clear cell carcinoma; PARP1, poly (ADP-Ribose) Polymerase 1; p53, tumor protein p53

CGA GCT GAG CGA-3' (forward) and 5'-TTA TAT TTC TTT CTG CAA GT-3' (reverse). The resulting 475-bp construct for Cav-1 was then cloned using a TopCloner TA Kit (Enzynomics, Daejeon, Korea) by excision at the EcoRI sites and then transferred into the expression plasmid pcDNA3.1(-) in the sense orientation (Thermo Fisher Scientific, Waltham, MA, USA) using T4 DNA ligase (NEB, Ipswich, MA, USA). Human ACE2 plasmid (pCEP4-myc-ACE2) was a gift from Erik Procko (Addgene plasmid no. 141185; <http://n2t.net/addgene:141185>; RRID: Addgene\_141185) (Chan et al., 2020).

#### Transient and stable transfection

OCCC cells were transfected with a specific plasmid using jetPRIME (Polyplus Transfection, New York, NY, USA) according to the manufacturer's instructions, in accordance with our previous studies (Park et al., 2020). A pMX-GFP vector (Cell Biolabs, Inc.,

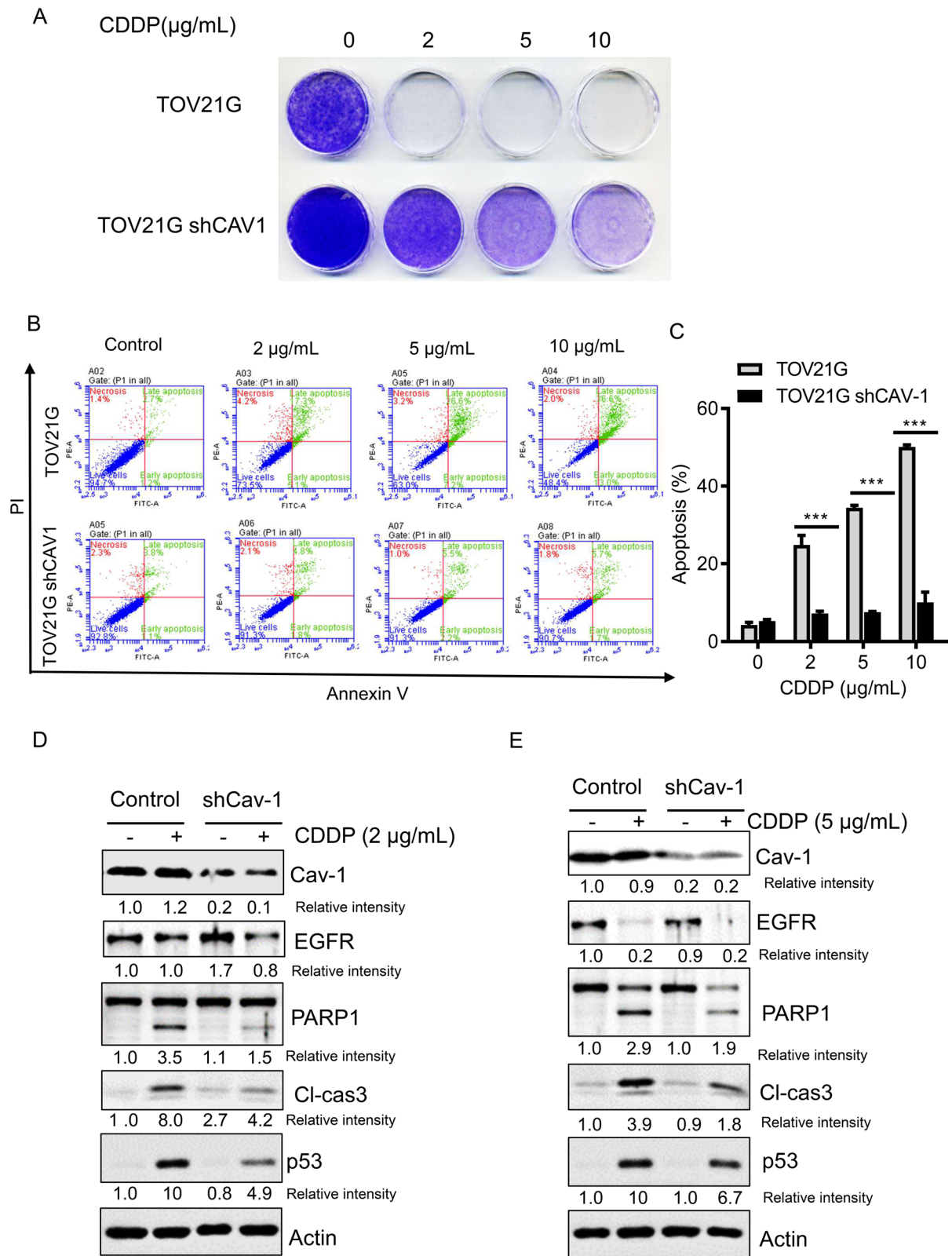
San Diego, CA, USA) was used to confirm the transfection efficiency. To induce transient expression of Cav-1 O/E, shCav-1, and shACE2, cells were transfected using jetPRIME. Subsequently, 4–5 h after transfection, cells were cultured in a fresh medium, followed by incubation for another 48 h. To create shCav-1-, Cav-1 O/E-, or shACE2-expressing stable cell lines, cells were transfected with respective plasmids using jetPRIME (Polyplus Transfection). After 48 h, transfected cells were subjected to selection for stable integrants by exposure to G418 (Life Technologies, Carlsbad, CA, USA) or hygromycin in a complete medium containing 10% FBS. The selection was performed until monolayer colonies were formed. The stable cell lines were then maintained in a medium supplemented with 10% FBS and G418 or hygromycin (LPS Solution Co., Ltd., Daejeon, Korea).

#### Western blot analysis

OCCC cells were incubated with the indicated concentrations of cisplatin for 24 h and were harvested for analysis. Briefly, cells were washed three times with ice-cold phosphate buffer and then lysed with lysis buffer (1% (w/v) SDS, 1.0 mM sodium orthovanadate, and 10 mM Tris (pH 7.4)). The protein was separated by electrophoresis and transferred to a polyvinylidene difluoride membrane (Pall Corporation, New York City, NY, USA). After blocking, the membrane was incubated with primary antibodies including Cav-1, EGF, p65, p-p65, and actin (Santa Cruz Biotechnology, Santa Cruz, CA, USA) overnight at 4 °C. After three times washing with TBST, the membrane was incubated with a secondary antibody and detected using pico-enhanced peroxidase (ELPIS Biotech, Daejeon, Korea).

#### Reverse transcription real-time PCR (qPCR)

Total RNA was extracted using RiboEX™ reagent (GeneAll Biotech, Seoul, Korea) according to the manufacturer's protocol. An equal amount of RNA (3  $\mu\text{g}$ ) from each sample was reverse transcribed into cDNA using a TOPscript™ RT DryMIX kit (Enzynomics, Seoul, Korea). SYBR® Green was used in qPCR as the fluorescent reporter dye to detect amplified cDNA using a Rotor-Gene Q thermal cycler (Qiagen, Hilden, Germany). The primers used in the present study are listed in Supplementary Information (Supplementary



◀**Fig. 2** Cav-1 silencing in TOV21G cells promotes resistance to cisplatin. **A** For clonogenic cell survival assay, TOV21G cells stably harboring a Cav-1 shRNA were treated with vehicle or cisplatin at indicated concentrations for 24 h. After washing, the cells were cultured in a fresh medium for 8 to 12 days and stained with crystal violet. Representative images are shown. **B, C** TOV21G shCav-1 cells were treated with vehicle or indicated concentrations of CDDP for 24 h and stained with annexin V–fluorescein isothiocyanate (FITC) and propidium iodide (PI). The proportion of apoptotic cells was measured using BD Accuri™ C6 Plus flow cytometer, and data are shown as the mean  $\pm$  standard deviation (SD) (\*\* $p < 0.001$  vs. vehicle group). **D, E** TOV21G shCav-1 cells were treated with vehicle or 2 and 5  $\mu\text{g}/\text{mL}$  cisplatin for 24 h, and total cell lysates were subjected to immunoblotting analysis. Representative images are shown. Cav-1, caveolin 1; Cl-cas3, cleaved caspase-3; EGFR, epidermal growth factor receptor; PARP1, poly (ADP-Ribose) polymerase 1; p53, tumor protein p53

Table 1). All experiments were conducted in three replicates to ensure statistical significance, and each independent experimental set was repeated two or three times. The comparative Ct method was used to quantify the relative gene expression. The number of PCR cycles (Ct) required for the SYBR® Green fluorescence intensity to exceed a threshold level immediately above the background was calculated for test and reference reactions. GAPDH was used as an endogenous control in all experiments. The results were analyzed by quantification relative to values for control cells.

#### Flow cytometry

OCCC cells were incubated with CDDP at the indicated concentrations for 24 h; next, cells were collected, washed with cold PBS, and centrifuged. Apoptotic cells were detected using FITC Annexin V Apoptosis Detection Kit I (no. 556547, BD Pharmingen, San Diego, CA, USA) according to the manufacturer's protocol. Briefly, cells were stained with 5  $\mu\text{L}$  of Annexin V-FITC, following which 5  $\mu\text{L}$  of propidium iodide (PI) and 400  $\mu\text{L}$  of annexin V-binding buffer were added to 100  $\mu\text{L}$  of cell suspension for 15 min. Flow cytometry was performed and analyzed using BD Accuri™ C6 Plus software ver1.0.23.1 (BD Biosciences).

#### Confocal and immunofluorescence microscopy

Briefly, OCCC cells were seeded and incubated for 24 h, fixed with 100% ice-cold methanol for 5 min

at room temperature, and then blocked with 1% bovine serum albumin (BSA) in PBS for 30 min. Next, cells were incubated with primary antibodies at a dilution ratio of 1:250 in a buffer (1% BSA in PBS) overnight at 4 °C and washed with PBS three times. Subsequently, cells were incubated with Alexa Fluor ®594 goat anti-rabbit IgG (H + L) (Invitrogen, Carlsbad, CA, USA) and goat anti-mouse IgG-h + l DyLight® 488 conjugated (Bethyl Laboratories Inc., Montgomery, TX, USA) at room temperature for 2 h. After washing three times with PBS, cells were counterstained with 500 ng/mL DAPI (absorbance at 405 nm) in PBS for 5 min. For immunofluorescence, images were captured using a Nikon Imaging System (NIS) Elements BR 4.60 system (Nikon, Tokyo, Japan). Confocal images were acquired with an Olympus FV1000 confocal microscope (Olympus, Tokyo, Japan) using single-line excitation (488 nm for anti-mouse antibodies, or 546 or 596 nm for anti-rabbit antibodies) or multitrack sequential excitation (488 nm and 633 nm). Images were analyzed by using the FV10-ASW software.

#### Luciferase assay

The luciferase assay was performed as previously described (Park et al., 2020). Briefly, OCCC cells were lysed with passive lysis buffer (Promega, Madison, WI, USA), and supernatants were collected by centrifugation at  $12,000 \times g$  for 15 min. Luciferase activity was measured using a Model TD-20/20 dual-mode luminometer (Turner BioSystems, Sunnyvale, CA, USA), and the *firefly* luciferase enzyme activity was normalized to *Renilla* luciferase activity.

#### Statistical analysis

All statistical analyses were done using GraphPad Prism 5.04 (GraphPad Software, Inc., San Diego, CA, USA). To compare between two groups, a student's *t*-test was used. For multiple groups comparison, data were subjected to analysis of variance, and pairwise comparisons were performed using the Student–Newman–Keuls post hoc method. All data presented in this study are expressed as the mean  $\pm$  standard deviation (SD).  $p < 0.05$  value was considered statistically significant.

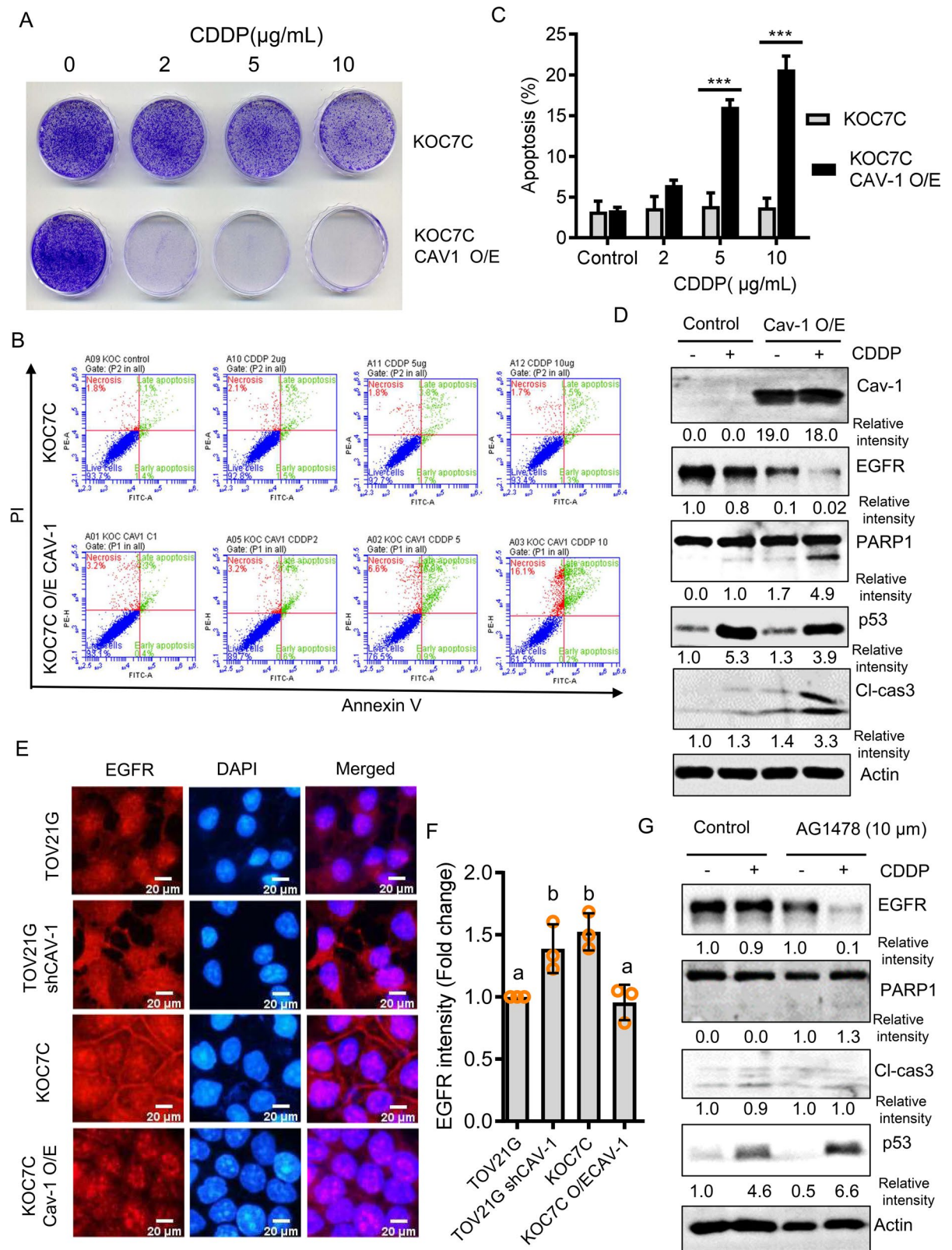




**Fig. 3** Overexpression of Cav-1 in KOC7C cells promotes sensitivity to cisplatin. **A** For clonogenic cell survival assay, Cav-1-overexpressing KOC7C cells were treated with vehicle or cisplatin at indicated concentrations for 24 h. After washing, the cells were cultured in a fresh medium for 8 to 12 days and stained with crystal violet. Representative images are shown. **B, C** Cav-1-overexpressing KOC7C cells were treated with vehicle or indicated concentrations of CDDP for 24 h and stained with annexin V–fluorescein isothiocyanate (FITC) and propidium iodide (PI). The proportion of apoptotic cells was measured using BD Accuri™ C6 Plus flow cytometer, and data are shown as the mean  $\pm$  standard deviation (SD) (\*\* $p < 0.001$  vs. vehicle group). **D** Cav-1-overexpressing KOC7C cells were treated with vehicle or 10  $\mu\text{g}/\text{mL}$  cisplatin for 24 h, and total cell lysates were subjected to immunoblotting analysis. Representative images are shown. **E** OCCC cells were fixed, permeabilized, and then stained with primary antibody against EGFR at a dilution of 1:250, followed by incubation with respective secondary antibodies at a dilution of 1:250. Then, cells were counterstained with DAPI and analyzed by immunofluorescence microscopy. **F** The relative quantitative value of EGFR expression. Fluorescence intensity was quantified using ImageJ software, and data are shown as the mean  $\pm$  standard deviation (SD) ( $n = 3$ ). Different letters over each bar represent significant differences between groups ( $p < 0.05$  using one-way ANOVA with the Newman–Keuls post hoc test). **G** KOC7C cells were pretreated with AG1478 (10  $\mu\text{m}$ ) for 2 h and then treated with vehicle or 10  $\mu\text{g}/\text{mL}$  cisplatin for 24 h; total cell lysates were subjected to immunoblotting analysis. Representative images are shown. Cav-1, caveolin 1; Cl-cas3, Cleaved Caspase-3; EGFR, epidermal growth factor receptor; OCCC, ovarian clear cell carcinoma; PARP1, Poly (ADP-Ribose) Polymerase 1; p53, tumor protein p53

## Results

Cav-1 expression in OCCC cells is inversely associated with sensitivity to CDDP

We evaluated the prognostic patterns of ovarian cancer in response to Cav-1 levels using clinical transcriptome datasets. Compared with the low Cav-1 expression group, patients with high Cav-1 expression displayed favorable prognosis (Fig. 1A (GSE26193), B (GSE63885), and Supplementary Fig. 1A [GSE27651]). To determine the clinical significance of Cav-1, we measured *CAV-1* mRNA expression in OVA and OCCC using a clinical transcriptome dataset (GSE29450 and GSE14407, respectively). Cav-1 expression was significantly lower in OVA and OCCC tissues than in normal ovarian tissues (Fig. 1C and D, respectively). To elucidate the cellular roles of Cav-1 in ovarian cancer, four OCCC cell lines, RMG-1, KOC7C, OVTOKO, TOV21G, and ES2 cells, were compared considering different readouts.

ES2, OVTOKO, and TOV21G cells showed relatively higher protein levels of Cav-1 than RMG-1 and KOC7C cells (Fig. 1E). However, since the ES2 cell line is known to partly display characteristic features of serous carcinoma (SC) (Kwok et al., 2014), it was excluded from further analyses. Next, four OCCC cell lines were exposed to CDDP, a representative front-line chemotherapeutic drug, at various concentrations (0–50  $\mu\text{g}/\text{mL}$ ) to compare cellular chemoresponses. KOC7C cells exhibited relatively higher resistance to CDDP treatment than other cell lines, whereas TOV21G cells showed greater drug susceptibility than other cells (Fig. 1F). The  $\text{IC}_{50}$  values of CDDP were 49.7, 319.5, 21.85, and 6.65  $\mu\text{g}/\text{mL}$  for RMG-1, KOC7C, OVTOKO, and TOV21G cells, respectively (Supplementary Fig. 1B and 1C). Notably, KOC7C cells were highly resistant to CDDP-induced apoptotic cell death (Supplementary Fig. 1C). As Cav-1-high cells showed greater chemosensitivity than Cav-1-low cells, we hypothesized that Cav-1 could be involved in mediating chemoresponses in OCCC. As shown in Fig. 1G and H, TOV21G cells displayed significantly higher levels of CDDP-induced apoptosis than KOC7C cells. Furthermore, CDDP treatment markedly increased caspase-3 activation and subsequent PARP-1 cleavage in TOV21G cells (Fig. 1I). Moreover, clonogenic assay results confirmed that more KOC7C cells than TOV21G cells survived after CDDP treatment (Fig. 1J). Collectively, these findings revealed that OCCC cells with high Cav-1 levels had increased sensitivity to CDDP-induced cell death.

Cav-1 improves the chemoresponses of OCCC cells

Next, we provided further molecular evidence indicating the involvement of Cav-1 in chemosensitivity. Cav-1 silencing using shRNA constructs (shCav-1) increased the number of TOV21G cell colonies after CDDP treatment (Fig. 2A). Indeed, genetic ablation of *CAV-1* in TOV21G cells led to significant resistance to CDDP-induced cell death in a dose-dependent manner, indicating Cav-1-mediated susceptibility to chemotherapy (Fig. 2B and C). Biochemically, treatment with 2  $\mu\text{g}/\text{mL}$  and 5  $\mu\text{g}/\text{mL}$  CDDP considerably diminished caspase-3 (Cl-cas3) activation and subsequent PARP-1 cleavage (Fig. 2D and E). Thus, Cav-1-deficient cells displayed attenuated levels of cell death signaling-related components, including PARP-1, cleaved caspase 3, and p53, suggesting that

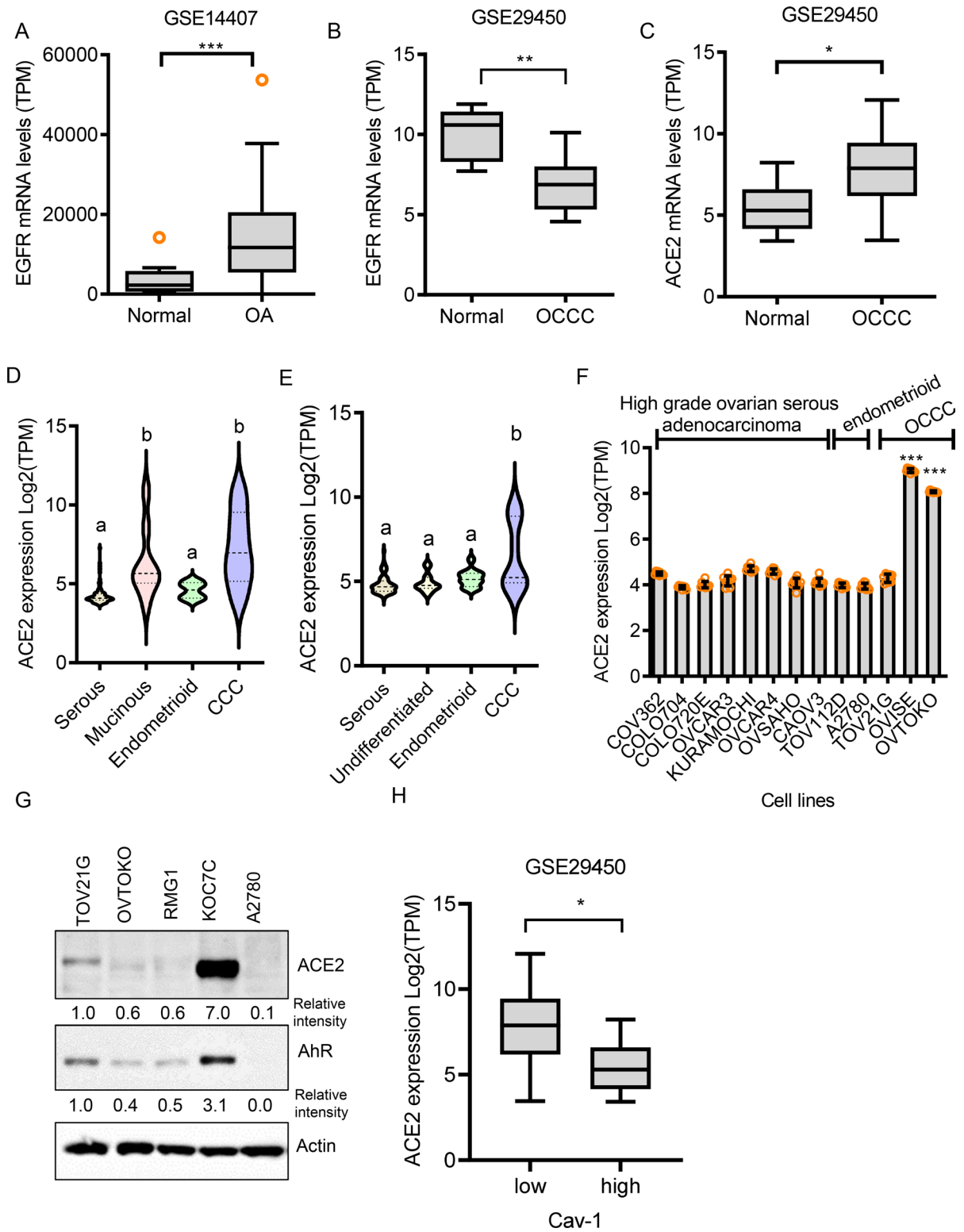


**Fig. 4** ACE2 expression in OCCC tissues and cells. **A** *EGFR* mRNA expression profiles of ovarian adenocarcinoma (OVA) and normal ovarian tissue were obtained from the GSE14407 dataset (normal,  $n=12$ ; OVA,  $n=12$ ). Asterisks (\*) indicate significant differences ( $***p<0.001$ ) compared with the normal group. **B, C** *EGFR* and *ACE2* mRNA expression profiles of OCCC and normal ovarian tissue were obtained from the GSE29450 dataset (normal,  $n=10$ ; OCCC,  $n=10$ ). Asterisks (\*) indicate significant differences ( $*p<0.05$ ;  $**p<0.01$ ) compared with the normal group. **D, E** ACE2 expression in different ovarian cancer types obtained from GSE26193 (**D**,  $n=107$ ) and GSE63885 (**E**,  $n=101$ ) datasets, respectively. **F** Ovarian cancer cell line-based transcriptomic analysis of ACE2 mRNAs from the GSE50831 dataset ( $n=189$ ). **G** Basal protein expression of ACE2 and AhR in OCCC cell lines was determined by immunoblotting analysis. **H** Ten samples with the highest Cav-1 expression and ten samples with the lowest Cav-1 expression were further evaluated for ACE2 levels. Results are shown as the mean  $\pm$  standard deviation (SD), and asterisks (\*) indicate significant differences between groups ( $*p<0.05$ ). ACE2, angiotensin-converting enzyme 2; AhR, aryl hydrocarbon receptor; Cav-1, caveolin 1; OCCC, ovarian clear cell carcinoma; EGFR, epidermal growth factor receptor

Cav-1 facilitates susceptibility to CDDP in TOV21G OCCC cells.

Based on the assumption that Cav-1 mediates chemosensitivity in OCCC cells, we examined the responses of Cav-1-low KOC7C cells to CDDP treatment. According to the colony-forming assay results, exogenous Cav-1 expression improved the chemoresponses of KOC7C cell colonies to CDDP treatment, although control KOC7C cells exhibited drug resistance (Fig. 3A). Moreover, the evaluation using annexin V-FITC/PI double-labeled staining revealed that Cav-1 overexpression increased apoptotic cell death in response to CDDP (Fig. 3B and C). Consistent with these results, Cav-1 overexpression enhanced caspase-3 activation and subsequent PARP-1 cleavage in CDDP-treated KOC7C cells (Fig. 3D), indicating the potential involvement of Cav-1 in mediating sensitivity to CDDP in KOC7C OCCC cells. These findings confirmed a positive association between Cav-1 and chemosensitivity in OCCC cells.

Cav-1-counteracted EGFR signaling is not involved in chemoresistance in OCCC cells

EGFR is a promising signaling platform in association with caveolae (Park et al., 2020), and the interaction between Cav-1 and EGFR can suppress kinase activity or protein stability of EGFR (Couet

et al., 1997, Park et al., 2020). Thus, in the present study, the effects of Cav-1 on EGFR were assessed in OCCC cells. Immunofluorescence revealed that Cav-1 silencing enhanced EGFR expression in TOV21G cells, while the overexpression of Cav-1 suppressed EGFR expression (Fig. 3E and F), indicating that Cav-1 is a negative regulator of EGFR expression. Next, the chemotherapeutic responses associated with EGFR signaling were evaluated. Unexpectedly, the suppression of EGFR expression using AG1478, a selective EGFR inhibitor, failed to improve sensitivity to CDDP in KOC7C and TOV21G cells (Fig. 3G and Supplementary Fig. 2A, 2B, and 2C), indicating that Cav-1-counteracted EGFR signaling was not involved in regulating sensitivity to CDDP in OCCC cells.

We further evaluated the prognosis patterns of ovarian cancer in response to EGFR levels using clinical transcriptome datasets. Patients with high EGFR expression displayed poor prognosis compared with those with low EGFR levels (GSE63885,  $p<0.001$ ; GSE27651,  $p<0.01$ , Supplementary Fig. 2D and 2E). Moreover, the gene expression profiles of patients with ovarian cancer revealed that OVA tissues exhibited significantly higher EGFR levels than normal ovarian tissues (Fig. 4A). Conversely, EGFR expression was downregulated in OCCC tissues compared with normal tissues (Fig. 4B). Collectively, our results showed that although Cav-1 counteracted EGFR expression, EGFR was not involved in modulating chemoresistance to CDDP in OCCC cells.

Cav-1 counteracts ACE2 expression in OCCC cells

As mentioned in the “Introduction,” caveolae and ACE2 can serve as crucial stress signaling platforms in several pathophysiological states as well as the entry of certain viruses, such as SARS-CoV-2. In contrast to EGFR, ACE2 levels were elevated in OCCC tissues compared with normal ovarian tissues (Fig. 4C). Compared with ACE2 levels in serous, endometrioid, and undifferentiated ovarian cancers, OCCC displayed elevated ACE2 expression (Fig. 4D and E) (GSE26193 ( $n=107$ ) and GSE63885 ( $n=101$ )). Based on ovarian cancer cell line-based transcriptomic database analysis, some OCCC cell lines tended to display relatively high ACE2 mRNA expression compared with serous and endometrioid

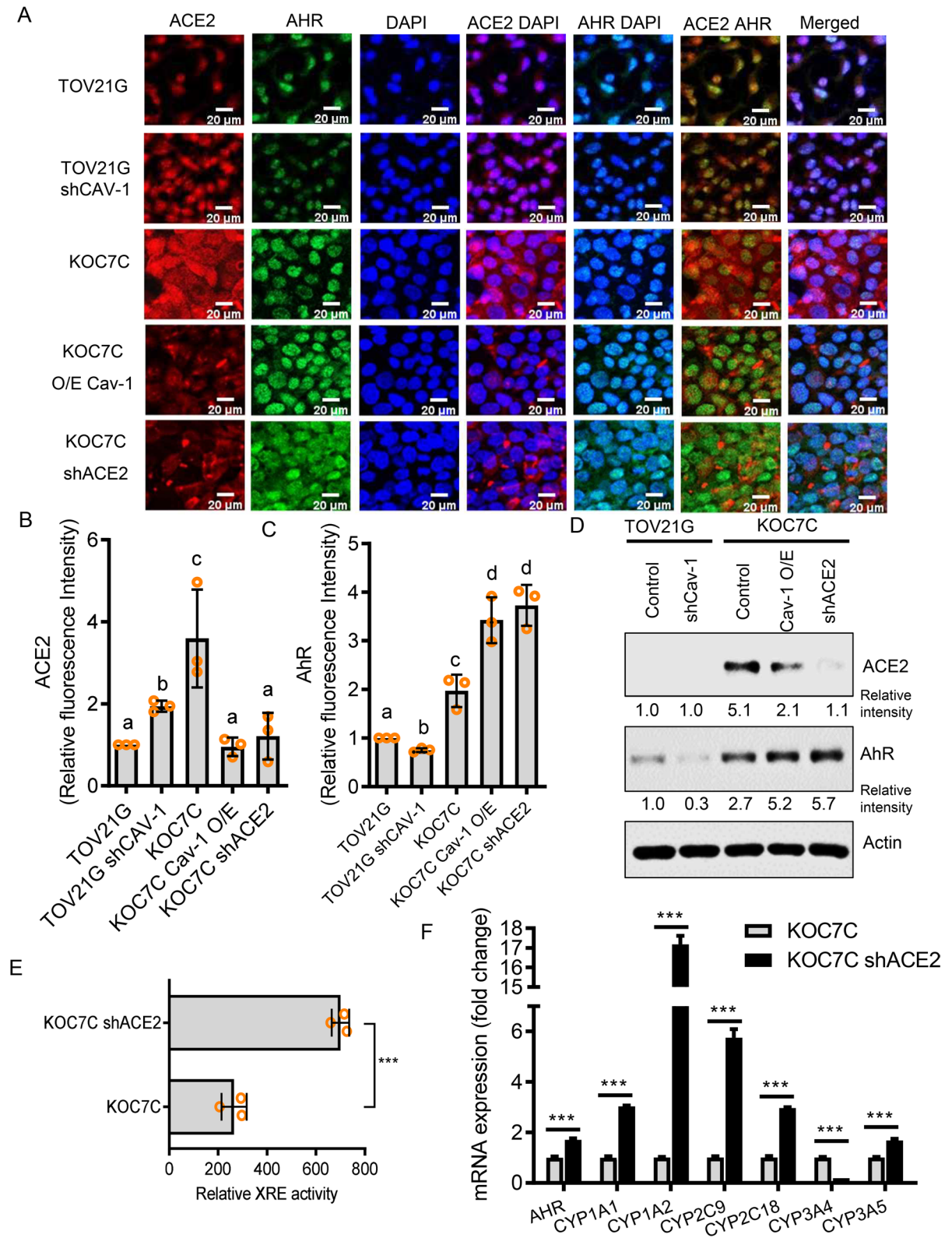


**Fig. 5** Cav-1 counteracts ACE2 expression in OCCC cells. **A** OCCC cells were fixed, permeabilized, and then stained with primary antibodies against ACE2 and AhR at a dilution of 1:250, followed by incubation with respective secondary antibodies at a dilution of 1:250. Then, cells were counterstained with DAPI and analyzed using confocal microscopy. **B** The relative quantitative value of ACE2 expression. **C** The relative quantitative value of AhR expression. Fluorescence intensity was quantified using ImageJ software, and data are shown as the mean  $\pm$  standard deviation (SD) ( $n=3$ ), and different lowercase letters (a–d) over each bar represent significant differences between groups ( $p<0.05$ ). **D** Total cell lysates from OCCC cells were subjected to immunoblotting analysis. Representative images are shown. **E** KOC7C and KOC7C shACE2 cells were transfected with basic-xenobiotic response element (Basic-XRE)-linked reporter plasmid for 24 h, and then, cell lysates were assessed for luciferase activity. Results are shown as the mean  $\pm$  SD, and asterisks represent a significant difference between groups ( $n=3$ ,  $***p<0.001$ ). **F** mRNA levels in KOC7C and KOC7C shACE2 cells were determined by quantitative real-time PCR (qPCR). Results are shown as the mean  $\pm$  SD, and asterisks represent a significant difference between groups ( $n=3$ ,  $***p<0.001$ ). ACE2, angiotensin-converting enzyme 2; AhR, aryl hydrocarbon receptor; Cav-1, caveolin 1; OCCC, ovarian clear cell carcinoma

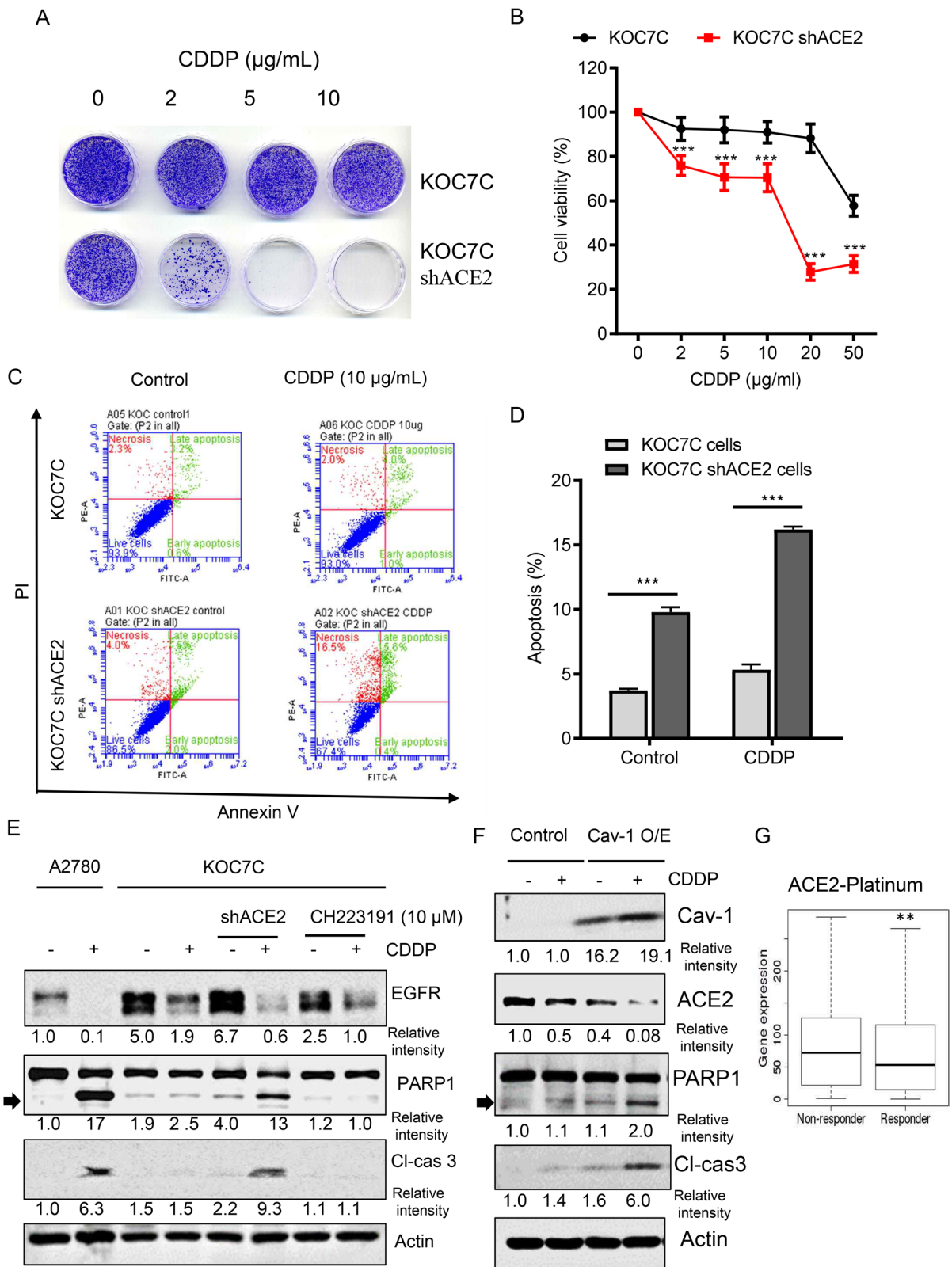
ovarian cancer cell lines (Fig. 4F: GSE50831,  $n=189$ ). Moreover, comparing protein levels, Cav-1-low KOC7C cells exhibited the highest ACE2 expression among the examined OCCC cells and the A2780 endometrioid ovarian cancer cell line (Fig. 4G). In addition to ACE2, AhR is a stress sensor that controls the expression of genes involved in pathological responses to internal and external insults (Stejskalova et al., 2011; Yan et al., 2018) and can mediate ACE2 regulation in pathogenic states (Lv et al., 2021). However, the AhR levels were not significantly altered in OCCC tissues (Supplementary Fig. 3A), and no tissue-specific patterns in *AhR* mRNA expression were detected in OCCC cell lines (Supplementary Fig. 3B) (GSE50831,  $n=189$ ). However, the results of the clinical transcriptomic analysis demonstrated that in patients with OCCC, tissues displaying high Cav-1 expression tended to have low ACE2 levels (Fig. 4H). Therefore, ACE2 was evaluated as a robust regulatory receptor in Cav-1-mediated signaling in OCCC.

To further elucidate the mechanism through which Cav-1 regulates ACE2 or AhR in OCCC cells, we examined protein localization using confocal microscopy. In KOC7C cells, Cav-1 overexpression inhibited ACE2 expression and increased AhR expression (Fig. 5A, B, C). In contrast, shRNA-induced Cav-1 deficiency enhanced ACE2 levels

and downregulated AhR expression in TOV21G cells (Fig. 5A, B, C). Furthermore, ACE2 deficiency upregulated AhR expression in KOC7C cells, suggesting that ACE2 counteracts AhR expression (Fig. 5C and D). Several epidemiological studies have reported that xenobiotic-responsive AhR regulates cytochrome P450 (CYP) enzymes and is strongly linked to cancer initiation and progression (Deuster et al., 2019; Feng et al., 2013). To further address the effects of ACE2 on AhR-mediated signaling of xenobiotic metabolism, xenobiotic response element (XRE)-linked transcription was evaluated in KOC7C OCCC cells. Notably, ACE2 knockdown markedly enhanced XRE-linked promoter activity (Fig. 5E), indicating that ACE2 counteracts AhR-linked promoter activity in OCCC cells. Furthermore, ACE2 participated in the downregulation of the AhR target gene expression, including *CYP1A1*, *CYP1A2*, *CYP2C9*, *CYP2C18*, and *CYP3A5* in KOC7C cells (Fig. 5F). Exceptionally, *CYP3A4* was positively regulated by ACE2 expression. Collectively, Cav-1 counteracted the expression of ACE2 whereas it was positively associated with the AhR expression and the subsequent transcriptional activation of xenobiotic metabolic enzymes except for *CYP3A4*.

Cav-1-counteracted ACE2 expression is involved in chemoresistance in OCCC cells

Considering functionality, we assessed whether Cav-1-counteracted ACE2 expression plays a role in modulating chemotherapeutic responses. Based on the results of the colony formation assay, suppression of *ACE2* expression improved the chemoresponse of KOC7C cell colonies to CDDP treatment; however, control KOC7C cells exhibited drug resistance (Fig. 6A). Expectedly, ACE2 knockdown significantly decreased KOC7C cell viability after CDDP treatment (Fig. 6B). Moreover, annexin V-FITC/PI double-labeled staining demonstrated that ACE2 suppression increased the proportion of apoptotic cells after CDDP treatment (Fig. 6C and D). Consistent with these results, ACE2 deficiency enhanced caspase-3 activation and subsequent PARP-1 cleavage in CDDP-treated KOC7C cells (Fig. 6E), indicating that ACE2 mediates CDDP resistance in KOC7C OCCC cells. However, blockade of AhR signaling using a selective inhibitor

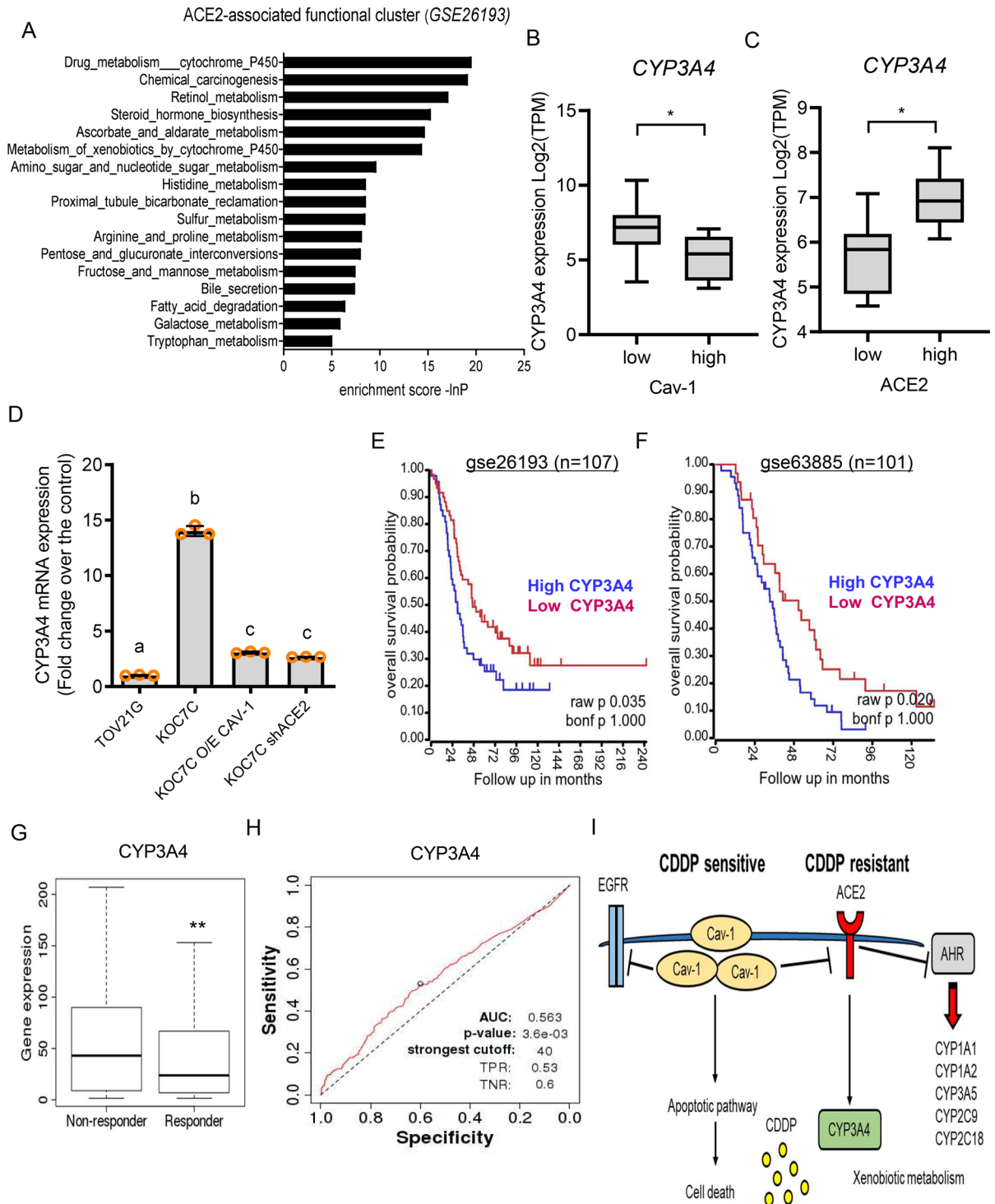


◀**Fig. 6** ACE2 silencing in KOC7C cells promotes sensitivity to cisplatin. **A** For clonogenic cell survival assay, ACE2-deficient KOC7C cells stably harboring ACE2 shRNA were treated with vehicle or cisplatin at indicated concentrations for 24 h. After washing, cells were cultured in a fresh medium for 8 to 12 days and stained with crystal violet. Representative images are shown. **B** KOC7C cells stably harboring ACE2 shRNA were treated with indicated concentrations of cisplatin for 24 h, and the MTT assay was performed. Results are shown as the mean  $\pm$  standard deviation (SD), and asterisks represent a significant difference from the KOC7C control cells at each cisplatin dose ( $n=3$ ,  $***p<0.001$ ). **C, D** shACE2-transfected KOC7C cells were treated with vehicle or 10  $\mu\text{g}/\text{mL}$  cisplatin for 24 h and stained with annexin V–fluorescein isothiocyanate (FITC) and propidium iodide (PI). The proportion of apoptotic cells was measured using BD Accuri™ C6 Plus flow cytometer, and data are shown as the mean  $\pm$  SD. Results are shown as the mean  $\pm$  SD, and asterisks represent a significant difference between groups ( $n=3$ ,  $***p<0.001$ ). **E** A2780 cells and shACE2-transfected KOC7C cells were treated with vehicle or 10  $\mu\text{g}/\text{mL}$  cisplatin for 24 h; KOC7C cells were co-incubated with CH223191 (10  $\mu\text{m}$ ) with or without 10  $\mu\text{g}/\text{mL}$  cisplatin for 24 h, and total cell lysates were subjected to immunoblotting analysis. **F** The control (the empty vector-transfected) and Cav-1-overexpressing KOC7C cells were treated with vehicle or 10  $\mu\text{g}/\text{mL}$  cisplatin for 24 h, and total cell lysates were subjected to immunoblotting analysis. Representative images are shown. ACE2, angiotensin-converting enzyme 2. **G** ACE2 levels in responders ( $n=752$ ) and non-responders ( $n=209$ ) to platinum treatment against ovarian cancer. Results are shown as a plot with Turkey whiskers, and asterisks (\*) indicate significant differences from the non-responder group ( $**p<0.01$ ). ACE2, angiotensin-converting enzyme 2; Cav-1, caveolin 1; Cl-cas3, Cleaved Caspase-3; EGFR, epidermal growth factor receptor; OCCC, ovarian clear cell carcinoma; PARP1, Poly (ADP-Ribose) polymerase 1

(CH223191) did not induce KOC7C cell apoptosis (Fig. 6E and Supplementary Fig. 3C and 3D). Furthermore, overexpression of Cav-1 inhibited ACE2 expression, which was concomitant with enhanced caspase-3 activation and subsequent PARP-1 cleavage in CDDP-treated KOC7C cells (Fig. 6F). On an assumption that ACE2 may increase chemoresistance, we tested the effects of exogenously introduced ACE2 on the TOV21G cells in response to CDDP treatment. However, ACE2 overexpression did not attenuate CDDP-induced apoptotic cell death in TOV21G cells (Supplementary Figs. 4A and 4B). Despite ACE2 overexpression, TOV21G maintained a high level of Cav-1, a key platform for chemosensitivity (Supplementary Fig. 4C). Based on clinical transcriptomic evaluation results, patients with low ACE2 mRNA expression exhibited better responses to platinum-based drugs than

those with high ACE2 mRNA expression ( $p<0.01$ ) (Fig. 6F). Overall, Cav-1-counteracted ACE2 expression plays a pivotal role in resistance to CDDP in KOC7C OCCC cells.

As a potent target of ACE2, CYP3A4A was positively regulated in OCCC cells under CDDP stress (Fig. 5F). CYP3A4 is a member of the CYP3A subfamily, the most abundant cytochrome P450 (P450) enzyme in the liver; more importantly, it is responsible for the metabolism of frontline chemotherapeutics, including platinum, resulting in drug clearance (Goldstein et al., 2013). According to clinical transcriptomic analysis results, ACE2-associated genes were notably involved in CYP-linked xenobiotic metabolism in patients with ovarian cancer (Fig. 7A, GSE26193,  $n=107$ ). In particular, tissues with high Cav-1 levels tended to display low CYP3A4 expression, whereas high ACE2 levels were linked to elevated CYP3A4 expression in patients with OCCC (Fig. 7B and C). These clinical tissue patterns were verified in OCCC cells. CYP3A4 mRNA expression was significantly higher in Cav-1-low/ACE2-high KOC7C cells than in Cav-1-high/ACE2-low TOV21G cells. Moreover, ACE2 deficiency and Cav-1 overexpression significantly decreased CYP3A4 levels in KOC7C cells (Fig. 7D). Accordingly, we postulated that Cav-1-counteracted ACE2 expression could facilitate CYP3A4 induction, contributing to chemoresistance and poor prognosis in patients. Moreover, patients with high CYP3A4 expression presented significantly shorter overall survival (OS) than patients with low CYP3A4 expression (Fig. 7E and F). Receiver operating characteristic (ROC) curve analysis results revealed that the patients with low CYP3A4 mRNA levels responded better to platinum-based drugs than those with high CYP3A4 mRNA expression ( $**p<0.01$ ) (Fig. 7G), demonstrating the excellent diagnostic value of CYP3A4 expression for ovarian cancer (Fig. 7H). Furthermore, patients with low CYP3A4 mRNA levels displayed better responses to taxane or the combination of platinum and taxane than those with high expression; however, CYP3A4 mRNA levels were not correlated with responses to other chemotherapeutic drugs (Supplementary Fig. 5). In summary, Cav-1-regulated ACE2 and its target CYP3A4 were positively associated with resistance to CDDP at the cellular level, leading to a poor prognosis.





◀**Fig. 7** CYP3A4 is positively correlated with ACE2 expression. **A** Clinical transcriptome-based functional analysis of ACE2-associated genes in patients with ovarian cancer (GSE26193,  $n=107$ ). **B, C** Ten samples with the highest Cav-1 expression and ten samples with the lowest Cav-1 expression were further evaluated for CYP3A4 levels. Results are shown as the mean  $\pm$  standard deviation (SD), and asterisks (\*) indicate significant differences between groups ( $*p<0.05$ ). **D** mRNA levels of CYP3A4 in OCCC cells were determined by quantitative real-time PCR (qPCR). Different lowercase letters over each bar represent significant differences between groups ( $p<0.05$  using one-way ANOVA with the Newman–Keuls post hoc test). **E, F** Kaplan–Meier plot of overall survival (OS) analysis for patients with low and high expression of CYP3A4 from the GSE26193 (**E**,  $n=107$ ) and GSE63885 datasets (**F**,  $n=101$ ). **G** CYP3A4 levels in responders ( $n=752$ ) and non-responders ( $n=209$ ) to platinum treatment against ovarian cancer. Results are shown as a plot with Turkey whiskers, and asterisks (\*) indicate significant differences from the non-responder group ( $**p<0.01$ ). **H** ROC curve for CYP3A4 levels in responders and non-responders to platin treatment. **I** A schematic diagram presenting mechanisms underlying Cav-1-ACE2 axis-linked modulation of chemosensitivity in OCCC cells. Cav-1 counteracts the expression of EGFR and ACE2 whereas it is positively associated with the expression of AhR and target CYPs except for CYP3A4. CYP3A4 is positively correlated with ACE2 expression and participates in the metabolic clearance of CDDP in patients with OCCC. ACE2, angiotensin-converting enzyme 2; AhR, aryl hydrocarbon receptor; AUC, area under the curve; Cav-1, caveolin 1; CDDP, cisplatin; OCCC, ovarian clear cell carcinoma; TPR, true positive rate; TNR, true negative rate

## Discussion

Although chemotherapeutic agents, such as platinum-based drugs, remain the standard first-line chemotherapy for treating ovarian cancer, chemoresistance is a major obstacle in treating various tumors, including OCCC. Caveolae respond to external stressors, including infectious agents and xenobiotic insults. As a primary component of caveolae, Cav-1 was assessed in terms of chemoresponses in OCCC cells. Notably, we observed that Cav-1 expression was inversely correlated with the chemoresistance in OCCC cells. Furthermore, Cav-1 counteracted EGFR and ACE2 expression. Notably, ACE2 positively regulated CYP3A4 expression, which is associated with CDDP clearance, attenuating pharmacological activity. Mechanistically, Cav-1 can control various signaling molecules (Liu et al., 2017; Vihanto et al., 2006) and acts as both a tumor suppressor and promoter (Belanger et al., 2004, Tirado et al., 2010b). It has been shown that Cav-1 expression is reduced in several cancer types such as ovarian and breast cancers

(Kai et al., 2001; Lee et al., 1998). However, the role of Cav-1 in the promotion, development, and chemoresistance of OCCC remains unclear. In the present study, high levels of Cav-1 indicated a favorable prognosis for ovarian cancer. Moreover, OCCC cells with high Cav-1 levels were more sensitive to CDDP treatment than those with low levels, and Cav-1 could improve sensitivity to CDDP. Similar to our results, Cav-1 overexpression mediates endocytosis and promotes the internalization of trastuzumab emtansine into HER-2-positive breast cancer cells (Chung et al., 2015). By contrast, Cav-1 mediates the chemoresistance of ovarian cancer by enhancing the Notch-1/Akt/NF- $\kappa$ B signaling pathways, attenuating the chemotherapy-induced cancer cell death (Zou et al., 2015). Likewise, Cav-1 promoted chemoresistance in Ewing’s sarcoma cells by activating phosphorylation of PKC $\alpha$  (Tirado et al., 2010b). These opposite actions of Cav-1 can be attributed to the unique characteristics of different cancer types as well as the distinct histological subtype of ovarian cancer under the different treatment regimes. In the case of OCCC, Cav-1 counteracted the expression of mediators responsible for chemoresistance or cancer cell proliferation. In particular, Cav-1-regulated ACE2 was an important mediator of the resistance to the platinum-based chemotherapeutic agents. Likewise, it is crucial to address what types of Cav-1-targeted mediators are involved in typical outcomes in response to the chemotherapeutic agents in different cancers.

In addition to ACE2, EGFR was negatively regulated by the Cav-1-linked signaling platform in the present study. EGFR has been deemed a potential prognostic biomarker and therapeutic target for ovarian cancer, given its reported expression in 30–98% of EOC (Gui, Shen, 2012, Niikura et al., 1997). Moreover, EGFR is an important signaling molecule that can interact with Cav-1, which critically regulates cell proliferation, migration, adhesion, and tumor angiogenesis by suppressing tyrosine phosphorylation and kinase activities (Couet et al., 1997, Vihanto et al., 2006, Williams et al., 2004). Additionally, radiation-induced Cav-1 is reportedly associated with Src kinase activity-dependent EGFR internalization and nuclear transport (Dittmann et al., 2008). Furthermore, EGFR tyrosine kinase inhibitors can suppress the growth of various cancer cell lines, including ovarian cancer (Ciardiello et al., 2001). Our recent study suggested a novel regulatory mechanism

of EGFR expression in the caveolar signaling scaffold (Park et al., 2020). Cav-1 triggers proteasome-mediated degradation of EGFR protein and counteracts the nuclear translocation of EGFR and subsequent EGFR-facilitated transcription of target genes. In the present study, Cav-1 was a negative regulator of EGFR, and patients with high EGFR expression exhibited a poor prognosis. Although Cav-1 counteracted EGFR expression, EGFR-mediated signaling did not participate in the chemosensitivity of OCCC cells. Moreover, EGFR levels were lower in OCCC tissues than in normal tissues. However, it is necessary to assess other underlying roles of EGFR-linked signaling during OCCC tumorigenesis and progression along with chemoresponses, while Cav-1 undoubtedly regulates EGFR expression in cells.

Unlike EGFR, chemoresistance was associated with elevated ACE2 expression in OCCC tissues. Previous studies have suggested that lipid raft microdomains and ACE2 can be crucial stress signaling platforms under various pathophysiological states as well as during the entry of some viruses, such as SARS-CoV-2 (Pelkmans, Helenius, 2003, Siczekarski, Whittaker, 2002). ACE2 plays a critical role in inhibiting cancer cell growth and overcoming chemoresistance in RCC (Khanna et al., 2021). Conversely, ACE2 inhibits angiogenesis through the vascular endothelial growth factor A/vascular endothelial growth factor receptor 2/extracellular signal-regulated protein kinase pathway (Zhang et al., 2019). Similarly, ACE2 overexpression potentially suppresses acquired platinum resistance-induced tumor angiogenesis in non-small-cell lung carcinoma (Cheng et al., 2016). In the present study, ACE2 downregulated the expression of AhR and that of its transcriptional targets—CYP1A1, CYP1A2, CYP2C9, CYP2C18, and CYP3A5—in KOC7C cells. In particular, AhR-induced CYP subfamily enzymes mostly mediate biotransformation into active clinical drugs (Zanger, Schwab, 2013). For instance, the antitumor agent, 5F-203, and its prodrug, Phortress, induce CYP1A1 expression by activating AhR signaling in IGROV-1 human ovarian cells, revealing enhanced sensitivity to these drugs via CYP-mediated metabolism (Hose et al., 2003). Although the attenuated activity of AhR signaling may reduce drug efficacy, ACE2 facilitated CYP3A4 expression regardless of AhR signaling, which potently contributes to the metabolic

clearance of platinum-based drugs. Among antitumor platinum complexes, CDDP and oxaliplatin display minimal inhibition of CYP2C9 activity in human liver microsomes (Masek et al., 2009). In the present study, the most prominent CYP in the Cav-1-ACE2 axis was CYP3A4, which facilitates the metabolic clearance and chemoresistance to platinum-based drugs. However, enhancing Cav-1 levels as a therapeutic target may counteract ACE2, enhance AhR transactivation and subsequent induction of the xenobiotic metabolic enzyme CYP genes, promote the antitumor activity of prodrugs, and/or suppress CYP3A4-mediated clearance of platinum-based drugs. Moreover, ACE2-mediated downregulation of AhR and CYP1A can alter hormonal activity, as CYP1A1 and CYP1A2 are involved in estrone metabolism via the oxidation of estrone to quinol and direct hydrolysis, respectively (Ohe et al., 2000; Yamazaki et al., 1998). Therefore, further investigations are needed to address the regulation of estrogen metabolism via Cav-1 and ACE2 signaling in ovarian cancer cells, in addition to drug metabolism.

In conclusion, we demonstrated that the Cav-1-ACE2 axis modulates chemosensitivity in OCCC cells. Mechanistically, Cav-1 counteracted ACE2 expression and subsequent transcription of CYPs. In addition, ACE2 was positively associated with the expression of CYP3A4, which is crucial for platinum-based drug clearance. Herein, our findings suggest that Cav-1 is a potent regulatory platform of sentinel signaling receptors, including ACE2 and AhR, during the progression of OCCC and chemotherapeutic responses in this disease. Overall, the integrative network between Cav-1 and ACE2 could be a promising predictive target of chemoresistance in treating OCCC. The biochemical signaling-based diagnostic decision could reduce the clinical burden and time for conventional therapy, providing new precision interventions against chemoresistant ovarian cancers.

**Author contribution** Arulkumar Nagappan: original draft, investigation, and formal analysis; Ki-Hyung Kim: visualization, clinical data analysis; Yuseok Moon: supervision, conceptualization, methodology, formal analysis, visualization, writing — review and editing.

**Funding** This research was supported by the Basic Science Research Program through the National Research Foundation

of Korea (NRF) funded by the Ministry of Science and ICT (NRF-2019R1A2C1084827).

**Data availability** Data is available on request from the authors. The data that support the findings of this study are available from the corresponding author upon reasonable request. Some data may not be made available because of privacy or ethical restrictions.

**Code availability** Not applicable.

#### Declarations

**Ethics approval** Not applicable.

**Consent to participate** Not applicable.

**Consent for publication** Not applicable.

**Competing interests** The authors declare no competing interests.

#### References

- Belanger MM, Roussel E, Couet J. Caveolin-1 is down-regulated in human lung carcinoma and acts as a candidate tumor suppressor gene. *Chest*. 2004;125(5):106s-s. [https://doi.org/10.1378/chest.125.5\\_suppl.106S](https://doi.org/10.1378/chest.125.5_suppl.106S).
- Cai C, Chen J. Overexpression of caveolin-1 induces alteration of multidrug resistance in Hs578T breast adenocarcinoma cells. *Int J Cancer*. 2004;111(4):522–9. <https://doi.org/10.1002/ijc.20300>.
- Chan KK, Dorosky D, Sharma P, Abbasi SA, Dye JM, Kranz DM, et al. Engineering human ACE2 to optimize binding to the spike protein of SARS coronavirus 2. *Science*. 2020;369(6508):1261–5. <https://doi.org/10.1126/science.abc870>.
- Chen HL, Fan LF, Gao J, Ouyang JP, Zhang YX. Differential expression and function of the caveolin-1 gene in non-small cell lung carcinoma. *Oncol Rep*. 2011;25(2):359–66. <https://doi.org/10.3892/or.2010.1095>.
- Cheng Q, Zhou L, Zhou J, Wan H, Li Q, Feng Y. ACE2 overexpression inhibits acquired platinum resistance-induced tumor angiogenesis in NSCLC. *Oncol Rep*. 2016;36(3):1403–10. <https://doi.org/10.3892/or.2016.4967>.
- Chung YC, Kuo JF, Wei WC, Chang KJ, Chao WT. Caveolin-1 dependent endocytosis enhances the chemosensitivity of HER-2 positive breast cancer cells to trastuzumab emtansine (T-DM1). *Plos One*. 2015;10(7):e0133072. <https://doi.org/10.1371/journal.pone.0133072>.
- Ciardello F, Caputo R, Bianco R, Damiano V, Fontanini G, Cuccato S, et al. Inhibition of growth factor production and angiogenesis in human cancer cells by ZD1839 (Iressa), a selective epidermal growth factor receptor tyrosine kinase inhibitor. *Clin Cancer Res*. 2001;7(5):1459–65.
- Couet J, Sargiacomo M, Lisanti MP. Interaction of a receptor tyrosine kinase, EGF-R, with caveolions. Caveolin binding negatively regulates tyrosine and serine/threonine kinase activities. *J Biol Chem*. 1997;272(48):30429–38. <https://doi.org/10.1074/jbc.272.48.30429>.
- Deuster E, Mayr D, Hester A, Kolben T, Zeder-Goss C, Burges A, et al. 2019 Correlation of the aryl hydrocarbon receptor with FSHR in ovarian cancer patients. *Int J Mol Sci*. 20(12). doi: <https://doi.org/10.3390/ijms20122862>.
- Dittmann K, Mayer C, Kehlbach R, Rodemann HP. Radiation-induced caveolin-1 associated EGFR internalization is linked with nuclear EGFR transport and activation of DNA-PK. *Mol Cancer*. 2008;7:69. <https://doi.org/10.1186/1476-4598-7-69>.
- Feng S, Cao Z, Wang X. Role of aryl hydrocarbon receptor in cancer. *Biochim Biophys Acta*. 2013;1836(2):197–210. <https://doi.org/10.1016/j.bbcan.2013.05.001>.
- Fujimoto T, Kogo H, Nomura R, Une T. Isoforms of caveolin-1 and caveolar structure. *J Cell Sci*. 2000;113(Pt 19):3509–17.
- Goldstein I, Rivlin N, Shoshana OY, Ezra O, Madar S, Goldfinger N, et al. Chemotherapeutic agents induce the expression and activity of their clearing enzyme CYP3A4 by activating p53. *Carcinogenesis*. 2013;34(1):190–8. <https://doi.org/10.1093/carcin/bgs318>.
- Gui T, Shen K. The epidermal growth factor receptor as a therapeutic target in epithelial ovarian cancer. *Cancer Epidemiol*. 2012;36(5):490–6. <https://doi.org/10.1016/j.canep.2012.06.005>.
- Gupta R, Toufaily C, Annabi B. Caveolin and cavin family members: dual roles in cancer. *Biochimie*. 107 Pt B:188–202. doi: <https://doi.org/10.1016/j.biochi.2014.09.010>.
- Hennighausen L, Lee HK. Activation of the SARS-CoV-2 Receptor Ace2 by cytokines through pan JAK-STAT enhancers. *SSRN*. 2020:3601827. doi: <https://doi.org/10.2139/ssrn.3601827>.
- Ho CC, Kuo SH, Huang PH, Huang HY, Yang CH, Yang PC. Caveolin-1 expression is significantly associated with drug resistance and poor prognosis in advanced non-small cell lung cancer patients treated with gemcitabine-based chemotherapy. *Lung Cancer*. 2008;59(1):105–10. <https://doi.org/10.1016/j.lungcan.2007.07.024>.
- Ho CM, Huang YJ, Chen TC, Huang SH, Liu FS, Chang Chien CC, et al. Pure-type clear cell carcinoma of the ovary as a distinct histological type and improved survival in patients treated with paclitaxel-platinum-based chemotherapy in pure-type advanced disease. *Gynecol Oncol*. 2004;94(1):197–203. <https://doi.org/10.1016/j.ygyno.2004.04.004>.
- Hose CD, Hollingshead M, Sausville EA, Monks A. Induction of CYP1A1 in tumor cells by the antitumor agent 2-[4-amino-3-methylphenyl]-5-fluoro-benzothiazole: a potential surrogate marker for patient sensitivity. *Mol Cancer Ther*. 2003;2(12):1265–72.
- Kai WC, Diatchenko L, Agoulnik A, Scharff KM, Schober H, Arlt K, et al. Caveolin-1 is down-regulated in human ovarian carcinoma and acts as a candidate tumor suppressor gene. *Am J Pathol*. 2001;159(5):1635–43. [https://doi.org/10.1016/S0002-9440\(10\)63010-6](https://doi.org/10.1016/S0002-9440(10)63010-6).
- Khanna P, Soh HJ, Chen CH, Saxena R, Amin S, Naughton M, et al. ACE2 abrogates tumor resistance to VEGFR

- inhibitors suggesting angiotensin-(1–7) as a therapy for clear cell renal cell carcinoma. *Sci Transl Med.* 13(577). doi: <https://doi.org/10.1126/scitranslmed.abc0170>.
- Kim HJ, Yoon A, Ryu JY, Cho YJ, Choi JJ, Song SY, et al. c-MET as a potential therapeutic target in ovarian clear cell carcinoma. *Sci Rep.* 2016;6:38502. <https://doi.org/10.1038/srep38502>.
- Krishnan B, Torti FM, Gallagher PE, Tallant EA. Angiotensin-(1–7) reduces proliferation and angiogenesis of human prostate cancer xenografts with a decrease in angiogenic factors and an increase in sFlt-1. *Prostate.* 2013;73(1):60–70. <https://doi.org/10.1002/pros.22540>.
- Kwok ALM, Wong OGW, Wong ESY, Tsun OKL, Chan KK, Cheung ANY. Caution over use of ES2 as a model of ovarian clear cell carcinoma. *J Clin Pathol.* 2014;67(10):921–2. <https://doi.org/10.1136/jclinpath-2014-202430>.
- Lee SW, Reimer CL, Oh P, Campbell DB, Schnitzer JE. Tumor cell growth inhibition by caveolin re-expression in human breast cancer cells. *Oncogene.* 1998;16(11):1391–7. <https://doi.org/10.1038/sj.onc.1201661>.
- Liu SL, Premont RT, Singh S, Rockey DC. Caveolin 1 and G-protein-coupled receptor kinase-2 coregulate endothelial nitric oxide synthase activity in sinusoidal endothelial cells. *Am J Pathol.* 2017;187(4):896–907. <https://doi.org/10.1016/j.ajpath.2016.11.017>.
- Lv JD, Yu P, Wang ZF, Deng W, Bao LL, Liu JN, et al. ACE2 expression is regulated by AhR in SARS-CoV-2-infected macaques. *Cell Mol Immunol.* 2021;18(5):1308–10. <https://doi.org/10.1038/s41423-021-00672-1>.
- Masek V, Anzenbacherova E, Machova M, Brabec V, Anzenbacher P. Interaction of antitumor platinum complexes with human liver microsomal cytochromes P450. *Anti-cancer Drugs.* 2009;20(5):305–11. <https://doi.org/10.1097/cad.0b013e328323a7a8>.
- Niikura H, Sasano H, Sato S, Yajima A. Expression of epidermal growth factor-related proteins and epidermal growth factor receptor in common epithelial ovarian tumors. *Int J Gynecol Pathol.* 1997;16(1):60–8. <https://doi.org/10.1097/00004347-199701000-00010>.
- Ohe T, Hirobe M, Mashino T. Novel metabolic pathway of estrone and 17 beta-estradiol catalyzed by cytochrome P-450. *Drug Metab Dispos.* 2000;28(2):110–2.
- Orezzoli JP, Russell AH, Oliva E, Del Carmen MG, Eichhorn J, Fuller AF. Prognostic implication of endometriosis in clear cell carcinoma of the ovary. *Gynecol Oncol.* 2008;110(3):336–44. <https://doi.org/10.1016/j.ygyno.2008.05.025>.
- Park SH, Kim J, Moon Y. Caveolar communication with xenobiotic-stalled ribosomes compromises gut barrier integrity. *Commun Biol.* 2020;3(1):270. <https://doi.org/10.1038/s42003-020-0994-1>.
- Pelkmans L, Helenius A. Insider information: what viruses tell us about endocytosis. *Curr Opin Cell Biol.* 2003;15(4):414–22. [https://doi.org/10.1016/s0955-0674\(03\)00081-4](https://doi.org/10.1016/s0955-0674(03)00081-4).
- Rothberg KG, Heuser JE, Donzell WC, Ying YS, Glenney JR, Anderson RG. Caveolin, a protein component of caveolae membrane coats. *Cell.* 1992;68(4):673–82. [https://doi.org/10.1016/0092-8674\(92\)90143-z](https://doi.org/10.1016/0092-8674(92)90143-z).
- Safe S, Lee SO, Jin UH. Role of the aryl hydrocarbon receptor in carcinogenesis and potential as a drug target. *Toxicol Sci.* 2013;135(1):1–16. <https://doi.org/10.1093/toxsci/kft128>.
- Scripture CD, Sparreboom A, Figg WD. Modulation of cytochrome P450 activity: implications for cancer therapy. *Lancet Oncol.* 2005;6(10):780–9. [https://doi.org/10.1016/S1470-2045\(05\)70388-0](https://doi.org/10.1016/S1470-2045(05)70388-0).
- Shajahan AN, Wang AF, Decker M, Minshall RD, Liu MC, Clarke R. Caveolin-1 tyrosine phosphorylation enhances paclitaxel-mediated cytotoxicity. *J Biol Chem.* 2007;282(8):5934–43. <https://doi.org/10.1074/jbc.M608857200>.
- Sieczkarski SB, Whittaker GR. Dissecting virus entry via endocytosis. *J Gen Virol.* 2002;83(Pt 7):1535–45. <https://doi.org/10.1099/0022-1317-83-7-1535>.
- Stejskalova L, Dvorak Z, Pavek P. Endogenous and exogenous ligands of aryl hydrocarbon receptor: current state of art. *Curr Drug Metab.* 2011;12(2):198–212. <https://doi.org/10.2174/138920011795016818>.
- Sugiyama T, Kamura T, Kigawa J, Terakawa N, Kikuchi Y, Kita T, et al. Clinical characteristics of clear cell carcinoma of the ovary: a distinct histologic type with poor prognosis and resistance to platinum-based chemotherapy. *Cancer.* 2000;88(11):2584–9.
- Tirado OM, MacCarthy CM, Fatima N, Villar J, Mateo-Lozano S, Notario V. Caveolin-1 promotes resistance to chemotherapy-induced apoptosis in Ewing's sarcoma cells by modulating PKCalpha phosphorylation. *Int J Cancer.* 2010a;126(2):426–36. <https://doi.org/10.1002/ijc.24754>.
- Tirado OM, MacCarthy CM, Fatima N, Villar J, Mateo-Lozano S, Notario V. Caveolin-1 promotes resistance to chemotherapy-induced apoptosis in Ewing's sarcoma cells by modulating PKC alpha phosphorylation. *Int J Cancer.* 2010b;126(2):426–36. <https://doi.org/10.1002/ijc.24754>.
- Vihanto MM, Vindis C, Djonov V, Cerretti DP, Huynh-Do U. Caveolin-1 is required for signaling and membrane targeting of EphB1 receptor tyrosine kinase. *J Cell Sci.* 2006;119(11):2299–309. <https://doi.org/10.1242/jcs.02946>.
- Wang Z, Wang N, Li W, Liu P, Chen Q, Situ H, et al. Caveolin-1 mediates chemoresistance in breast cancer stem cells via beta-catenin/ABCG2 signaling pathway. *Carcinogenesis.* 2014;35(10):2346–56. <https://doi.org/10.1093/carcin/bgu155>.
- Williams TM, Medina F, Badano I, Hazan RB, Hutchinson J, Muller WJ, et al. Caveolin-1 gene disruption promotes mammary tumorigenesis and dramatically enhances lung metastasis in vivo. Role of Cav-1 in cell invasiveness and matrix metalloproteinase (MMP-2/9) secretion. *J Biol Chem.* 2004;279(49):51630–46. <https://doi.org/10.1074/jbc.M409214200>.
- Xu J, Agyemang S, Qin Y, Aysola K, Giles M, Oprea G, et al. 2014 A novel pathway that links caveolin-1 down-regulation to BRCA1 dysfunction in serous epithelial ovarian cancer cells. *Enliven Chall Cancer Detect Ther.* 1(1). doi: <https://doi.org/10.18650/2376-046x.11004>.
- Yamazaki H, Shaw PM, Guengerich FP, Shimada T. Roles of cytochromes P450 1A2 and 3A4 in the oxidation of estradiol and estrone in human liver microsomes. *Chem Res Toxicol.* 1998;11(6):659–65. <https://doi.org/10.1021/tx970217f>.

- Yan B, Liu S, Shi Y, Liu N, Chen L, Wang X, et al. Activation of AhR with nuclear IKK $\alpha$  regulates cancer stem-like properties in the occurrence of radioresistance. *Cell Death Dis.* 2018;9(5):490. <https://doi.org/10.1038/s41419-018-0542-9>.
- Zanger UM, Schwab M. Cytochrome P450 enzymes in drug metabolism: regulation of gene expression, enzyme activities, and impact of genetic variation. *Pharmacol Ther.* 2013;138(1):103–41. <https://doi.org/10.1016/j.pharmthera.2012.12.007>.
- Zhang Q, Lu S, Li T, Yu L, Zhang Y, Zeng H, et al. ACE2 inhibits breast cancer angiogenesis via suppressing the VEGFa/VEGFR2/ERK pathway. *J Exp Clin Cancer Res.* 2019;38(1):173. <https://doi.org/10.1186/s13046-019-1156-5>.
- Zou W, Ma XD, Hua W, Chen BL, Cai GQ. Caveolin-1 mediates chemoresistance in cisplatin-resistant ovarian cancer cells by targeting apoptosis through the Notch-1/Akt/NF-kappa B pathway. *Oncol Rep.* 2015;34(6):3256–63. <https://doi.org/10.3892/or.2015.4320>.

**Publisher's Note** Springer Nature remains neutral with regard to jurisdictional claims in published maps and institutional affiliations.